

# A new approach to the integration of rotational motion in systems with interacting rigid bodies

Igor P. Omelyan

*Institute for Condensed Matter Physics, National Ukrainian Academy of Sciences,  
1 Svientsitsky st., UA-290011 Lviv, Ukraine. E-mail: nep@icmp.lviv.ua*

(June 15, 2021)

**MSC numbers:** 65C20; 65-04; 68U20; 70E15; 82A71

**Keywords:** Numerical methods; Motion of rigid bodies; Long-time integration; Molecular dynamics simulation; Polyatomic molecules; Machine computation

*A running head:*

Numerical integration of rigid-body motion

Dr. I. P. Omelyan

Institute for Condensed Matter Physics

National Ukrainian Academy of Sciences

1 Svientsitsky st., UA-290011 Lviv

UKRAINE

Tel/Fax: +380-322-761978

E-mail: nep@icmp.lviv.ua

## Abstract

A new approach is developed to integrate numerically the equations of motion for systems of interacting rigid polyatomic molecules. With the aid of a leapfrog framework, we directly involve principal angular velocities into the integration, whereas orientational positions are expressed in terms of either principal axes or quaternions. As a result, the rigidity of molecules appears to be an integral of motion, despite the atom trajectories are evaluated approximately. The algorithm derived is free of any iterative procedures and it allows to perform both energy- and temperature-conserving simulations. The corresponding integrators are time reversible but the symplectic behavior is only achieved in mean. Symplectic versions are also described. They provide the conservation of volume in phase space precisely at each time step and, moreover, lead to exact solutions for angular velocities in the inertial-motion regime. It is shown that the algorithm exhibits excellent stability properties and conserves the energy even somewhat better than the atomic-constraint technique.

## I. INTRODUCTION

A lot of theories in physical chemistry treats the liquid as a system of classical rigid bodies. The method of molecular dynamics (MD) remains the main tool for investigation of such a model. An important problem in MD simulations is the development of stable and efficient algorithms for integrating the equations of motion with orientational degrees of freedom. The straightforward parameterization of these degrees, Euler angles, is very inefficient for numerical calculations because of singularities inherent in the description [1–3]. Within singularity free approaches, the orientations of molecules typically are expressed in terms of quaternions [4–6]. High-order Gear methods were utilized to integrate the rigid-body equations of motion in early investigations [7–10]. These schemes are not reversible or symplectic, and it is not clear that the extra order obtained is relevant, since they quickly become exhibit poor long-term stability of energy with increasing the step size [5, 11].

Various alternatives to the Gear approach have been proposed and implemented over the years. These include Verlet [12], velocity Verlet [13], leapfrog [14], and Beeman [15] integrators, which are based on the Störmer central difference approximation [7, 16] of accelerations. Such integrators proved to be the most efficient, because high accuracy can be reached with minimal cost measured in terms of force evaluations. The main problem with these methods is that they were initially constructed, in fact, to integrate translational motion assuming the velocity-independence of the accelerations, and, therefore, additional modifications are necessary to use them for rotational dynamics.

In the atomic approach [17–21], the parameterization of orientational degrees of freedom is circumvented by involving individual Cartesian coordinates of atomic sites. As a result, the Verlet algorithm and its velocity versions appear to be directly applicable. The dynamics is determined by integrating the equations of motion for these sites, subject to constraints that the intramolecular bond distances are fixed. Until now, the great majority of MD simulations on polyatomics are performed using the atomic-constraint technique due to its exceptional long-time stability. Although this approach can be applied, in principle, to arbitrary systems including the case of flexible molecules, it has some disadvantages. For example, to exactly reproduce the

rigid molecular structure, complicated systems of nonlinear equations are needed to be solved by iterations at each time step of the integration process. In general, the convergence is not guaranteed [22] and looping becomes possible already at relatively small step sizes, especially for macromolecules with bond angle reactions. An additional complexity arises for point molecules with embedded multipoles, since then the forces are not easily decomposable into direct site-site contributions.

In order to obviate these difficulties, Ahlrichs and Brode have devised a hybrid method [23] in which the principal axes of molecules are considered as pseudo particles and constraint forces are introduced to maintain their orthonormality. The principal axes were evaluated within the Verlet framework via a recursive procedure which does not solve exactly the constraint equations to convergence, but instead writes the rotational matrix as an exponential for sum of some anti-symmetric matrices, restricting by a finite number of terms. It was established, however, that the exponential propagation leads to much worse results on energy conservation than those obtained in the atomic-constraint technique. Recently, acting in the spirit of the pseudo-particle formalism, a leapfrog-like algorithm has also been proposed [24]. In this algorithm the entire rotation matrix and the corresponding conjugate momentum are treated as dynamical variables, and the matrix of constrain forces is evaluated exactly. In such a way, the lost precision was reproduced, but this required again to find iterative solutions to highly nonlinear equations. Moreover, since velocities do not appear explicitly, it is hard to extend the pseudo-particle approach to thermostatted versions.

The first efforts on adopting the Störmer group of integrators to rotational motion in its pure form were done by Fincham [25–26]. As a result, explicit and implicit angular-momentum leapfrog algorithms have been introduced. In the case of a more accurate implicit version, the system of four nonlinear equations per molecule is solved iteratively for the same number of quaternion components [26]. As was soon realized [27], the Fincham’s algorithms are not very efficient in energy-conserving simulations, given that the artificial rescaling procedure is used to maintain the unit quaternion norm, and additional transformations with approximately computed rotational matrices and angular momenta are necessary to evaluate the principal components of angular velocities. The question of how to replace the crude renormalization by a more natural procedure has been considered too [28]. As a consequence, the quaternion dynamics

with constraints was formulated within the velocity Verlet framework. Similar ideas were used to adopt the pseudo-particle approach to velocity-Verlet and Beeman integrators [27]. It has been shown that such algorithms conserve the total energy better with respect to the implicit leapfrog integrator [26] but worse than the atomic-constraint method, especially in the case of long-duration simulations with large step sizes.

Among other techniques developed in recent years it is necessary to mention the multiple time scale (MTS) integration [29-34]. The reversible reference system propagator (RESP) algorithm by Berne *at al.* [32] is a general approach which yields a whole family of MTS integrators. The basic idea of this approach lies in using a short time step for the rapidly varying fast forces, and a large time step for the nonbonding slow forces arising from the interactions at long interparticle distances. Then the most time-consuming slow forces will be recalculated less frequently than in usual methods, saving significantly the computer time. It is worth remarking that the RESP approach, being originally constructed on Cartesian coordinates, can be adapted [35] to orientational variables. There are some arguments to stay that a reformulation of the RESP approach within these variables can be more convenient for applications (see Sec. IV). From this point of view, and taking into account that the fastest motions are handled (inside the innermost cycle with the least step size) using standard algorithms, the developing of methods for direct integration of orientational variables presents an interest in the context of the MTS approach as well.

Quite recently, to improve the efficiency of integration in orientational space, a new angular-velocity leapfrog algorithm has been proposed [36]. Its main advantages were the intrinsic conservation of rigid structures and high stability properties. However, a common drawback, inherent in all precise long-term integrators on rigid polyatomics, still remained, namely, the necessity to solve by iteration nonlinear equations.

In the present paper we develop the angular-velocity algorithm by avoiding any iterative procedures. A thermostatted version is also introduced. We demonstrate that the integrators derived are time reversible, symplectic and the total energy is conserved even better than within the atomic-constraint method. It is discussed that our approach can be especially useful for simulations of systems at high temperatures, where the inertial-motion regime plays an important role in rotational dynamics.

## II. ADVANCED LEAPFROG ALGORITHM

We shall deal with a classical collection of  $N$  rigid molecules composed of  $M$  point interaction sites. According to the molecular approach, the dynamics for such a system can be considered in view of translational and rotational motions. The translational motion is expressed in terms of the center of mass  $\mathbf{r}_i = \sum_{a=1}^M m_a \mathbf{r}_i^a / m$  of each molecule ( $i = 1, \dots, N$ ), where  $\mathbf{r}_i^a$  denotes the positions of atomic site  $a$  within molecule  $i$  and  $m = \sum_{a=1}^M m_a$  and  $m_a$  are the masses of a separate molecule and partial atoms, respectively. Then the translational part of time evolution can be determined by the first-order differential equations:  $d\mathbf{r}_i/dt = \mathbf{v}_i$  and  $m d\mathbf{v}_i/dt = \mathbf{f}_i$ , where  $\mathbf{f}_i = \sum_{j;a,b}^{N;M} \mathbf{f}_{ij}^{ab}(|\mathbf{r}_i^a - \mathbf{r}_j^b|)$  is the force acting on molecule  $i$  due to the site-site interactions  $\mathbf{f}_{ij}^{ab}$  with the other ( $j \neq i$ ) molecules and  $\mathbf{v}_i$  designates the center-of-mass velocity.

### A. Rotational motion in body-vector and quaternion representations

In the body-vector representation [4, 23, 27], the Cartesian coordinates of three principal axes  $XYZ$  of the molecule are assumed to be orientational variables. These variables can be collected into the  $3 \times 3$  orthonormal matrices  $\mathbf{A}_i$ , so that the site positions in the laboratory frame are:  $\mathbf{r}_i^a(t) = \mathbf{r}_i(t) + \mathbf{A}_i^+(t) \mathbf{\Delta}_a$ , where  $\mathbf{\Delta}_a = (\Delta_X^a, \Delta_Y^a, \Delta_Z^a)^+$  is a vector-column of these positions in the body frame attached to the molecule and  $\mathbf{A}^+$  denotes the matrix transposed to  $\mathbf{A}$ . The time-independent quantities  $\mathbf{\Delta}_a$  ( $a = 1, \dots, M$ ) are completely defined by the rigid molecular structure. The rate of change in time of orientational matrices can be given as

$$\frac{d\mathbf{A}_i}{dt} = \begin{pmatrix} 0 & \Omega_Z^i & -\Omega_Y^i \\ -\Omega_Z^i & 0 & \Omega_X^i \\ \Omega_Y^i & -\Omega_X^i & 0 \end{pmatrix} \mathbf{A}_i \equiv \mathbf{W}(\mathbf{\Omega}_i) \mathbf{A}_i, \quad (1)$$

where  $\Omega_X^i$ ,  $\Omega_Y^i$  and  $\Omega_Z^i$  are principal components of the angular velocity  $\mathbf{\Omega}_i$ , and  $\mathbf{W}$  is a skewsymmetric matrix associated with  $\mathbf{\Omega}_i$ , i.e.,  $\mathbf{W}^+(\mathbf{\Omega}_i) = -\mathbf{W}(\mathbf{\Omega}_i)$ .

In an alternative approach [4, 9], the matrix  $\mathbf{A}_i$  is a function,

$$\mathbf{A}(\mathbf{q}_i) = \begin{pmatrix} -\xi_i^2 + \eta_i^2 - \zeta_i^2 + \chi_i^2 & 2(\zeta_i \chi_i - \xi_i \eta_i) & 2(\eta_i \zeta_i + \xi_i \chi_i) \\ -2(\xi_i \eta_i + \zeta_i \chi_i) & \xi_i^2 - \eta_i^2 - \zeta_i^2 + \chi_i^2 & 2(\eta_i \chi_i - \xi_i \zeta_i) \\ 2(\eta_i \zeta_i - \xi_i \chi_i) & -2(\xi_i \zeta_i + \eta_i \chi_i) & -\xi_i^2 - \eta_i^2 + \zeta_i^2 + \chi_i^2 \end{pmatrix}, \quad (2)$$

of the four-component quaternion  $\mathbf{q}_i \equiv (\xi_i, \eta_i, \zeta_i, \chi_i)^+$ . The time derivatives of  $\mathbf{q}_i$  can be presented [36] in the form

$$\frac{d\mathbf{q}_i}{dt} = \frac{1}{2} \begin{pmatrix} 0 & \Omega_Z^i & -\Omega_X^i & -\Omega_Y^i \\ -\Omega_Z^i & 0 & -\Omega_Y^i & \Omega_X^i \\ \Omega_X^i & \Omega_Y^i & 0 & \Omega_Z^i \\ \Omega_Y^i & -\Omega_X^i & -\Omega_Z^i & 0 \end{pmatrix} \begin{pmatrix} \xi_i \\ \eta_i \\ \zeta_i \\ \chi_i \end{pmatrix} \equiv \frac{1}{2} \mathbf{Q}(\Omega_i) \mathbf{q}_i, \quad (3)$$

where  $\mathbf{Q}(\Omega_i)$  is a skewsymmetric matrix again. The normalization condition  $\mathbf{q}_i^2 = \xi_i^2 + \eta_i^2 + \zeta_i^2 + \chi_i^2 = 1$ , which ensures the orthonormality  $\mathbf{A}_i \mathbf{A}_i^+ = \mathbf{I}$  of  $\mathbf{A}_i \equiv \mathbf{A}(\mathbf{q}_i)$ , where  $\mathbf{I}$  designates the unit matrix, has been used to obtain Eq. (3).

The relations (1) and (3) for orientational coordinates need to be supplemented by the Euler's equations for angular velocities

$$\begin{aligned} J_X \frac{d\Omega_X^i}{dt} &= K_X^i + (J_Y - J_Z) \Omega_Y^i \Omega_Z^i, \\ J_Y \frac{d\Omega_Y^i}{dt} &= K_Y^i + (J_Z - J_X) \Omega_Z^i \Omega_X^i, \\ J_Z \frac{d\Omega_Z^i}{dt} &= K_Z^i + (J_X - J_Y) \Omega_X^i \Omega_Y^i, \end{aligned} \quad (4)$$

where  $J_\alpha$  denote the time-independent moments inertia of the molecule along its principal axes ( $\alpha = X, Y, Z$ ) and  $K_\alpha^i$  are body-frame components,  $\mathbf{K}_i = \mathbf{A}_i \mathbf{k}_i$ , of the torque  $\mathbf{k}_i = \sum_{j;a,b}^{N;M} (\mathbf{r}_i^a - \mathbf{r}_i) \times \mathbf{f}_{ij}^{ab}$  exerted on molecule  $i$  with respect to its center of mass.

## B. Evaluation of angular velocities and coordinates

Let  $\{\mathbf{r}_i(t), \mathbf{v}_i(t - \frac{h}{2}), \mathbf{S}_i(t), \Omega_i(t - \frac{h}{2})\}$  be an initial spatially-velocity configuration of the system, where the velocities and positions are defined on alternate half-time steps with  $h$  being the fixed step size and  $\mathbf{S}_i(t) \equiv \mathbf{A}_i(t)$  or  $\mathbf{q}_i(t)$  are the orientational coordinates for the principal-axis or quaternion representations, respectively. The translational variables can be integrated applying the usual [14] leapfrog algorithm

$$\begin{aligned} \mathbf{v}_i(t + \frac{h}{2}) &= \mathbf{v}_i(t - \frac{h}{2}) + h\mathbf{f}_i(t)/m + \mathcal{O}(h^3), \\ \mathbf{r}_i(t + h) &= \mathbf{r}_i(t) + h\mathbf{v}_i(t + \frac{h}{2}) + \mathcal{O}(h^3) \end{aligned} \quad (5)$$

in which forces  $\mathbf{f}_i(t)$  are explicitly evaluated in terms of known spatial coordinates  $\mathbf{r}_i(t)$  and  $\mathbf{S}_i(t)$ . As can be verified easily, expanding the left- and right-hand sides of both the



lines of Eq. (5) into Taylor series over  $h$ , the algorithm produces truncation single-step errors of order  $h^3$  in coordinates and velocities.

In the case of rotational motion it is not a simple matter to adopt the standard leapfrog scheme, since the principal angular accelerations are velocity-dependent and the time derivatives of orientational coordinates depend not only on the angular velocity but also on the coordinates themselves. These problems were handled previously by Fincham [26] in his angular-momentum versions of the leapfrog algorithm. Recently [27, 36], it was shown that more superior techniques follow when principal angular velocities are involved directly into the integration. Within the leapfrog framework, mid-step values for the angular velocities can be evaluated by writing

$$\Omega_\alpha^i(t + \frac{h}{2}) = \Omega_\alpha^i(t - \frac{h}{2}) + h \left[ K_\alpha^i(t) + (J_\beta - J_\gamma) \Omega_\beta^i(t) \Omega_\gamma^i(t) \right] / J_\alpha + \mathcal{O}(h^3), \quad (6)$$

where Euler equations (4) have been taken into account,  $(\alpha, \beta, \gamma)$  denote an array of three cyclic permutations for  $(X, Y, Z)$ , and torques  $K_\alpha^i(t)$  are computed via coordinates  $\mathbf{r}_i(t)$  and  $\mathbf{S}_i(t)$ . Equation (6) presents a rotational-motion analog for the first line of (5) but it must be complemented by an interpolation of the products of angular velocities to on-step levels of time. It is quite naturally to perform such an interpolation in the form

$$\Omega_\beta^i(t) \Omega_\gamma^i(t) = \frac{1}{2} \left[ \Omega_\beta^i(t - \frac{h}{2}) \Omega_\gamma^i(t - \frac{h}{2}) + \Omega_\beta^i(t + \frac{h}{2}) \Omega_\gamma^i(t + \frac{h}{2}) \right] + \mathcal{O}(h^2), \quad (7)$$

where  $\mathcal{O}(h^2)$  uncertainties are in the self-consistency with the second-order accuracy of angular-velocity propagation (6). In view of (7), vector expression (6) is an implicit equation with respect to  $\Omega_i(t + \frac{h}{2})$ , which allows to be solved by iteration [36].

Similarly to the translational-position evaluations (second line of Eq. (5)), we integrate orientational coordinates,

$$\mathbf{S}_i(t + h) = \mathbf{S}_i(t) + h \mathbf{H}_i(t + \frac{h}{2}) \mathbf{S}_i(t + \frac{h}{2}) + \mathcal{O}(h^3), \quad (8)$$

for the cases of principal-axis vectors ( $\mathbf{S}_i \equiv \mathbf{A}_i, \mathbf{H}_i \equiv \mathbf{W}_i$ ) and quaternion ( $\mathbf{S}_i \equiv \mathbf{q}_i, \mathbf{H}_i \equiv \frac{1}{2} \mathbf{Q}_i$ ) representations, where Eqs. (1) and (3) have been used. The matrices  $\mathbf{W}_i \equiv \mathbf{W}(\Omega_i)$  and  $\mathbf{Q}_i \equiv \mathbf{Q}(\Omega_i)$  are calculated in (8) using the already defined values of  $\Omega_i(t + \frac{h}{2})$ , whereas the obvious choice for mid-step values of orientational variables is

$$\mathbf{S}_i(t + \frac{h}{2}) = \frac{1}{2} [\mathbf{S}_i(t) + \mathbf{S}_i(t + h)] + \mathcal{O}(h^2). \quad (9)$$

Equations (8) and (9) constitute, in fact, a system of linear equations with respect to elements of  $\mathbf{A}_i(t + h)$  or  $\mathbf{q}_i(t + h)$ , which, is solved analytically,

$$\mathbf{S}_i(t + h) = [\mathbf{I} - \frac{h}{2}\mathbf{H}_i(t + \frac{h}{2})]^{-1}[\mathbf{I} + \frac{h}{2}\mathbf{H}_i(t + \frac{h}{2})]\mathbf{S}_i(t) + \mathcal{O}(h^3), \quad (10)$$

where it is understood that  $\mathbf{I}$  designates either three- or four-dimensional unit matrix in the principal-axis or quaternion domains, respectively.

Taking into account expressions (1) and (3) for matrix  $\mathbf{H}_i$ , the result (10) can be written more explicitly,

$$\begin{aligned} \mathbf{A}_i(t + h) &= \frac{\mathbf{I}[1 - \frac{h^2}{4}\Omega_i^2(t + \frac{h}{2})] + h\mathbf{W}_i + \frac{h^2}{2}\mathbf{P}_i}{1 + \frac{h^2}{4}\Omega_i^2(t + \frac{h}{2})} \mathbf{A}_i(t) \equiv \mathbf{D}_i(t, h) \mathbf{A}_i(t), \\ \mathbf{q}_i(t + h) &= \frac{\mathbf{I}[1 - \frac{h^2}{16}\Omega_i^2(t + \frac{h}{2})] + \frac{h}{2}\mathbf{Q}_i}{1 + \frac{h^2}{16}\Omega_i^2(t + \frac{h}{2})} \mathbf{q}_i(t) \equiv \mathbf{G}_i(t, h) \mathbf{q}_i(t), \end{aligned} \quad (11)$$

where  $[\mathbf{P}_i]_{\alpha\beta} = \Omega_\alpha^i \Omega_\beta^i$  denotes a symmetric matrix which, as the matrices  $\mathbf{W}_i$  and  $\mathbf{Q}_i$ , is computed in (11) using the angular velocities at middle-step time  $t + \frac{h}{2}$ . It can be checked that the matrix  $(\mathbf{I} - \epsilon\mathbf{H})^{-1}(\mathbf{I} + \epsilon\mathbf{H})$  is orthonormal at arbitrary values of  $\epsilon$ , provided  $\mathbf{H}^+ = -\mathbf{H}$ . As a result, the  $3 \times 3$  and  $4 \times 4$  evolution matrices  $\mathbf{D}_i$  and  $\mathbf{G}_i$  are orthonormal by construction as well. Using the equalities  $\mathbf{W}_i^2 = \mathbf{P}_i - \Omega_i^2\mathbf{I}$  and  $\mathbf{Q}_i^2 = -\Omega_i^2\mathbf{I}$ , these matrices can be presented in the exclusive compact form

$$\mathbf{D}_i(t, h) = \mathbf{exp}[\varphi_i \mathbf{W}_i / \Omega_i]_{t+\frac{h}{2}}, \quad \mathbf{G}_i(t, h) = \mathbf{exp}[\phi_i \mathbf{Q}_i / \Omega_i]_{t+\frac{h}{2}}, \quad (12)$$

where  $\varphi_i = \arcsin[h\Omega_i(t + \frac{h}{2}) / (1 + \frac{h^2}{4}\Omega_i^2(t + \frac{h}{2}))]$ ,  $\phi_i = \arcsin[h\Omega_i(t + \frac{h}{2}) / (2 + \frac{h^2}{8}\Omega_i^2(t + \frac{h}{2}))]$  and  $\mathbf{exp}$  designates the matrix exponential. Then it becomes clear that matrices  $\mathbf{D}_i$  and  $\mathbf{G}_i$  define three- and four-dimensional rotations on angles  $\varphi_i$  and  $\phi_i$  in the laboratory frame and quaternion space, respectively. In the first case the rotation is performed around the unit vector  $\mathbf{\Omega}_i / \Omega_i|_{t+\frac{h}{2}}$ , whereas in the second one it is carried out around a virtual orth which is perpendicular to all four orths of the quaternion space.

From the above, the following important statement emerges immediately. If initially the orthonormality of  $\mathbf{A}_i$  and the unit norm of  $\mathbf{q}_i$  are fulfilled, they will be satisfied perfectly in future, despite an approximate character of the evaluated trajectories. This excellent property distinguishes the algorithm introduced from all other singularity-free algorithms known, since no artificial or constraint normalizations as well as no recursive or iterative procedures are necessary to conserve the rigidness of molecules.

### C. Thermostatted dynamics

Since the velocities appear explicitly in our approach, it is possible to introduce various thermostats [37-43] to simulate the canonical ensemble. Usually [26, 44], thermostatted versions allow to perform simulations with greater step sizes than those used within the energy-conserving dynamics. In canonical MD simulations the time evolution should be determined in such a way to keep a fixed temperature  $T = \langle \mathcal{T} \rangle$  of the system, where  $\mathcal{T} = 2\Gamma/(lNk_B)$  and  $\Gamma$  are the instantaneous temperature and kinetic energy, respectively,  $k_B$  is the Boltzmann's constant, and  $\langle \rangle$  denotes the statistical averaging. The number  $l$  of degrees of freedom per particle is equal to six for arbitrary rigid polyatomics, except linear molecules when  $l = 5$ .

We shall consider here a N ose-Hoover thermostat [39-41], although the extension to others thermostats [37, 38, 43] can also be realized. According to the N ose-Hoover technique, the thermostatted dynamics is obtained introducing the generalized friction forces  $-\lambda m\mathbf{v}_i \equiv -\lambda\partial\Gamma/\partial\mathbf{v}_i$ . These virtual forces are added to the real ones and, as a result, the equations of motion for translational velocities transform into  $m d\mathbf{v}_i/dt = \mathbf{f}_i - \lambda m\mathbf{v}_i$ . In our case, when orientational degrees of freedom are present additionally, the kinetic energy consists of both translational and rotational parts,  $\Gamma = \frac{1}{2} \sum_{i=1}^N [m\mathbf{v}_i^2 + \sum_{\alpha}^{X,Y,Z} J_{\alpha} \Omega_{\alpha}^i{}^2]$ . This requires the introduction of friction torques,  $-\lambda\partial\Gamma/\partial\Omega_{\alpha}^i = -\lambda J_{\alpha} \Omega_{\alpha}^i$ , which should be taken into account in Euler equations (4). The time-dependent friction coefficient varies in time with the total excess of kinetic energy to its canonical mean value,

$$d\lambda/dt = (\mathcal{T} - T)/(T\tau^2), \quad (13)$$

and governs by a characteristic thermostat relaxation time  $\tau$ .

In the presence of friction forces, the translational velocities can be integrated applying a Toxvaerd leapfrog algorithm [45]. It is based on the estimation

$$\mathbf{v}_i(t) = \frac{1}{2}[\mathbf{v}_i(t - \frac{h}{2}) + \mathbf{v}_i(t + \frac{h}{2})] + \mathcal{O}(h^2) \quad (14)$$

of on-step velocities, commonly used to calculate a kinetic part of the total energy at time  $t$  in microcanonical simulations and to verify the energy conservation. Then adding the corresponding friction term  $\lambda(t)m\mathbf{v}_i(t)$  to the right-hand side of the first line of Eq. (5) and solving the obtained equation with respect to new mid-step translational velocities, one finds

$$\mathbf{v}_i(t + \frac{h}{2}) = \{[1 - \frac{h}{2}\lambda(t)]\mathbf{v}_i(t - \frac{h}{2}) + h\mathbf{f}_i(t)/m\}/[1 + \frac{h}{2}\lambda(t)]. \quad (15)$$

Quite analogously, in the case of rotational motion we use the estimation

$$\mathbf{\Omega}_i(t) = \frac{1}{2}[\mathbf{\Omega}_i(t - \frac{h}{2}) + \mathbf{\Omega}_i(t + \frac{h}{2})] + \mathcal{O}(h^2), \quad (16)$$

for on-step angular velocities, needed to computer the friction torques  $-\lambda(t)J_\alpha\Omega_\alpha^i(t)$ . These torques we add to the right-hand side of Eq. (6) which now can be presented in the following form

$$\Omega_\alpha^i(t + \frac{h}{2}) = \{[1 - \frac{h}{2}\lambda(t)]\Omega_\alpha^i(t - \frac{h}{2}) + h\mathcal{K}_\alpha^i(t)/J_\alpha\}/[1 + \frac{h}{2}\lambda(t)], \quad (17)$$

where

$$\mathcal{K}_\alpha^i(t) = K_\alpha^i(t) + \frac{1}{2}(J_\beta - J_\gamma) \left[ \Omega_\beta^i(t - \frac{h}{2})\Omega_\gamma^i(t - \frac{h}{2}) + \Omega_\beta^i(t + \frac{h}{2})\Omega_\gamma^i(t + \frac{h}{2}) \right]. \quad (18)$$

The vector equation (17) constitutes a system of three equations per molecule for the same number of unknowns  $\Omega_\alpha^i(t + \frac{h}{2})$  (note that  $\lambda(t)$  is known from the previous time step). As in the case of microcanonical evaluation ( $\lambda(t) \equiv 0$ ), the system can be solved iteratively, replacing initially  $\mathbf{\Omega}_i(t + \frac{h}{2})$  by  $\mathbf{\Omega}_i(t - \frac{h}{2})$  in all nonlinear terms which are collected in the right-hand side of (17). The calculated values of  $\mathbf{\Omega}_i(t + \frac{h}{2})$  are then considered as initial guess for the next iteration. The convergence of iterations is justified by the smallness of  $h$  which always is met in actual MD simulations.

Using the already defined translational and angular velocities, we evaluate the instantaneous mid-step temperature  $\mathcal{T}(t + \frac{h}{2}) \equiv \mathcal{T}(\{\mathbf{v}_i(t + \frac{h}{2}), \mathbf{\Omega}_i(t + \frac{h}{2})\})$ . Then equation (13) is integrated as follows [45]:

$$\lambda(t + h) = \lambda(t) + h[\mathcal{T}(t + \frac{h}{2}) - T]/(T\tau^2). \quad (19)$$

The coordinates  $\mathbf{S}_i(t + h)$  and  $\mathbf{r}_i(t + h)$  are updated according to the same transformations (see Eq. (11) and the second line of Eq. (5)) as for energy-conserving dynamics.

#### D. Avoidance of iterative procedures

An essential advantage of the approach presented lies in the fact that solutions to Eq. (17) (or (6)) can be obtained without applying any iterative procedures. First of all it is necessary to point out that the equations are nonlinear only when all the principal moments of inertia are different. Let us consider now this more difficult case (specific examples are described in Subsect. II F) and assume for definiteness that

$J_X < J_Y < J_Z$ . Then the first two unknowns  $\Omega_X(t + \frac{h}{2})$  and  $\Omega_Y(t + \frac{h}{2})$  are the most fast variables which should be excluded from the iterations to increase the convergence.

Such an excluding indeed can be carried out solving the first two ( $\alpha = X, Y$ ) equations of system (17) with respect to  $\Omega_X^i(t + \frac{h}{2})$  and  $\Omega_Y^i(t + \frac{h}{2})$ . The result is

$$\Omega_X^i(t + \frac{h}{2}) = \frac{\theta_X + h\rho_X\theta_Y\Omega_Z^i(t + \frac{h}{2})}{1 + h^2\mu^2\Omega_Z^i{}^2(t + \frac{h}{2})}, \quad \Omega_Y^i(t + \frac{h}{2}) = \frac{\theta_Y + h\rho_Y\theta_X\Omega_Z^i(t + \frac{h}{2})}{1 + h^2\mu^2\Omega_Z^i{}^2(t + \frac{h}{2})}, \quad (20)$$

where  $\theta_\alpha = \nu_- \Omega_\alpha^i(t - \frac{h}{2}) / \nu_+ + [K_\alpha^i(t) / (J_\alpha \nu_+) + \rho_\alpha \Omega_\beta^i(t - \frac{h}{2}) \Omega_\gamma^i(t - \frac{h}{2})] h$ ,  $\nu_\pm = 1 \pm \frac{h}{2} \lambda(t)$ ,  $\rho_\alpha = \sigma_\alpha / \nu_+$ ,  $\sigma_\alpha = (J_\beta - J_\gamma) / (2J_\alpha)$  and  $0 < \mu^2 = -\rho_X \rho_Y \leq 1 / (4\nu_+^2)$ . The last inequalities follow from the requirements  $J_\alpha > 0$  and  $J_\alpha \leq J_\beta + J_\gamma$  imposed on principal moments of inertia. It is worth remarking that putting formally  $\lambda(t) \equiv 0$ , i.e.  $\nu_\pm \equiv 1$ , we shall come to solutions of Eq. (6) corresponding to the microcanonical ensemble. In view of (20), only the third equation ( $\alpha = Z$ ) of system (17) really needs to be iterated with respect to one variable  $\Omega_Z^i(t + \frac{h}{2})$ . Since this variable is the most slow quantity, a well convergence will be guaranteed even for not so well normally behaved case as an almost linear body, when  $J_X \ll J_Y < J_Z$ .

Finally, we shall show how to obviate the iterative solutions at all. Substituting result (20) into the third equation of system (17) and presenting the  $Z$ -th component of angular velocity in the form  $\Omega_Z^i(t + \frac{h}{2}) = s_0 + \delta$  lead to the following algebraic equation

$$a_0 + a_1\delta + a_2\delta^2 + a_3\delta^3 + a_4\delta^4 + a_5\delta^5 = 0 \quad (21)$$

with the coefficients

$$\begin{aligned} a_0 &= (s_0 - \theta_Z) \vartheta_+^2 - h\rho_Z[\theta_X\theta_Y\vartheta_- + h(\rho_Y\theta_X^2 + \rho_X\theta_Y^2)s_0], \\ a_1 &= \vartheta_+ - h^2\{(\rho_Y\theta_X^2 + \rho_X\theta_Y^2)\rho_Z - \mu^2 s_0[(5s_0 - 4\theta_Z)\vartheta_+ + 2h\theta_X\theta_Y\rho_Z]\}, \\ a_2 &= h^2\mu^2[6s_0 - 2\theta_Z + h\rho_Z\theta_X\theta_Y + h^2\mu^2 s_0^2(10s_0 - 6\theta_Z)], \\ a_3 &= 2h^2\mu^2[1 + h^2\mu^2 s_0(5s_0 - 2\theta_Z)], \\ a_4 &= h^4\mu^4(5s_0 - \theta_Z), \quad a_5 = h^4\mu^4, \end{aligned} \quad (22)$$

where  $\vartheta_\pm = 1 \pm h^2\mu^2 s_0^2$ . Equation (21) is fifth order and the corresponding solutions for  $\Omega_Z^i(t + \frac{h}{2})$  are independent on parameter  $s_0$ , provided the unknown  $\delta$  is precisely determined. However, as is well known, only algebraic equations of fourth or less orders allow to be solved in quadratures.

To overcome this difficulty, it is necessary to choose the parameter  $s_0$  as a good prediction for  $\Omega_Z^i(t + \frac{h}{2})$  to be entitled to ignore the highest-order terms in the left-hand side of Eq. (21). The simplest choice for this can be found assuming that the nonlinear velocity term in the right-hand side of Eq. (18) at  $\alpha = Z$  is time-independent during the interval  $[t - \frac{h}{2}, t + \frac{h}{2}]$ , i.e., letting  $\Omega_X^i(t + \frac{h}{2})\Omega_Y^i(t + \frac{h}{2}) = \Omega_X^i(t - \frac{h}{2})\Omega_Y^i(t - \frac{h}{2}) + \mathcal{O}(h)$ . As a result, one obtains

$$s_0 = \theta_Z + h\rho_Z\Omega_X^i(t - \frac{h}{2})\Omega_Y^i(t - \frac{h}{2}) \quad (23)$$

that represents the original values of  $\Omega_Z^i(t + \frac{h}{2})$  with the second-order truncation error, so that  $\delta = \mathcal{O}(h^2)$ . It is easy to see that in this case the two last terms  $a_4\delta^4$  and  $a_5\delta^5$  in the left-hand side of Eq. (21) behaves as  $\mathcal{O}(h^{12})$  and  $\mathcal{O}(h^{14})$ , respectively. Taking into account the smallness of  $h$ , such terms can merely be omitted without any loss of the precision, because they involve uncertainties of order  $\mathcal{O}(h^{12})$  into the desired solution and appear to be too small with respect to third-order truncation errors  $\mathcal{O}(h^3)$  involved initially in angular velocities by the algorithm.

Eq. (21) is now transformed into the third-order algebraic equation

$$a_0 + a_1\delta + a_2\delta^2 + a_3\delta^3 = \mathcal{O}(h^{12}) \quad (24)$$

which can easily be solved analytically,

$$\begin{aligned} \delta_1 &= -\frac{1}{3}a_2/a_3 + c - b/c + \mathcal{O}(h^{12}), \\ \delta_{2,3} &= -\frac{1}{3}a_2/a_3 - \frac{1}{2}[c - b/c \pm i\sqrt{3}(c + b/c)] + \mathcal{O}(h^{12}), \end{aligned} \quad (25)$$

where  $b = \frac{1}{9}(3a_1a_3 - a_2^2)/a_3^2$ ,  $c = (d + \sqrt{b^3 + d^2})^{1/3}$  and  $d = \frac{1}{54}(9a_1a_2a_3 - 27a_0a_3^2 - 2a_2^3)/a_3^3$ . Among three solutions (25), only the first one  $\delta_1$  is real and satisfies the physical boundary condition  $\delta_1 \rightarrow h^2$  when  $h$  goes to zero (the other two solutions  $\delta_{2,3}$  are purely imaginary at  $h \rightarrow 0$  and they tend to infinity as  $\sim \pm i/h$ ). Thus, the desired  $Z$ -th component of the angular velocity is

$$\Omega_Z^i(t + \frac{h}{2}) = s_0 + \delta_1. \quad (26)$$

The rest two components  $\Omega_X^i(t + \frac{h}{2})$  and  $\Omega_Y^i(t + \frac{h}{2})$  are reproduced on the basis of equalities (20).

## E. Symplectic properties

It can be checked readily that past and future values of all the integrated quantities enter symmetrically into Eqs. (5)–(7), (10), (14)–(17) and (19). Therefore, the algorithm derived is time reversible with respect to translational and rotational motions and within both microcanonical and canonical ensembles. In order to investigate symplectic properties, it is necessary to choose arbitrary canonically conjugated coordinates, express them in terms of  $\mathbf{r}_i$ ,  $\mathbf{v}_i$ ,  $\mathbf{A}_i$  and  $\boldsymbol{\Omega}_i$ , and, then look whether the corresponding volume in phase space is conserved. We accept the positions  $\mathbf{r}_i^a = \mathbf{r}_i + \mathbf{A}_i^+ \boldsymbol{\Delta}_a$  and momenta  $\mathbf{p}_i^a = m_a(\mathbf{v}_i + \mathbf{A}_i^+ [\boldsymbol{\Omega}_i \times \boldsymbol{\Delta}^a])$  of atomic sites to be such canonical coordinates.

Since the translational and rotational variables are not coupled explicitly during our integration (in the microcanonical ensemble), the transitions from old to new values of the canonical coordinates, caused by varying these variables, can be considered separately at each time step. As is well known, the translational leapfrog algorithm (5) is symplectic, so that the corresponding transition will be performed with the unit Jacobian. In its turn, the time evolution of orientational variables can be split into two consequent transformations. During the first one, the principal angular velocities  $\boldsymbol{\Omega}_i$  are changed provided the orientational positions  $\mathbf{A}_i$  remain constant, whereas the second transformation will correspond to the change of  $\mathbf{A}_i$  at fixed values of  $\boldsymbol{\Omega}_i$  (a similar splitting is often used [46] to prove the symplecticity of usual schemes). As far as the orientational matrices  $\mathbf{A}_i$  appear to be always orthonormal ( $\det \mathbf{A}_i = 1$ ), the effect of their changes in time is reduced simply to a rotation of vectors  $\mathbf{r}_i^a - \mathbf{r}_i$  and  $\mathbf{p}_i^a - m_a \mathbf{v}_i$  in three-dimensional space. Thus, the second transformation is evidently volume preserving. Finally, since angular velocities  $\boldsymbol{\Omega}_i$  enter linearly into momenta  $\mathbf{p}_i^a$ , it can be shown that the first transformation will conserve the volume too provided the Jacobian  $\mathcal{J}_{\boldsymbol{\Omega}_i} = \det \boldsymbol{\Theta}_i$  is equal to unity, where  $\boldsymbol{\Theta}_i = \partial\{\Omega_X^i(t + \frac{h}{2}), \Omega_Y^i(t + \frac{h}{2}), \Omega_Z^i(t + \frac{h}{2})\} / \partial\{\Omega_X^i(t - \frac{h}{2}), \Omega_Y^i(t - \frac{h}{2}), \Omega_Z^i(t - \frac{h}{2})\}$ .

Partially differentiating each equation ( $\alpha = X, Y, Z$ ) of system (6) consequently over  $\Omega_X^i(t - \frac{h}{2})$ ,  $\Omega_Y^i(t - \frac{h}{2})$  and  $\Omega_Z^i(t - \frac{h}{2})$ , and solving the obtained three systems of linear equations with respect to nine elements of  $\boldsymbol{\Theta}_i$ , one finds

$$\mathcal{J}_{\boldsymbol{\Omega}_i} = \frac{[1 - h^2\{\sigma_Y\sigma_Z\Omega_X^i{}^2 + \sigma_X\sigma_Z\Omega_Y^i{}^2 + \sigma_X\sigma_Y\Omega_Z^i{}^2\} + 2h^3\sigma_X\sigma_Y\sigma_Z\Omega_X^i\Omega_Y^i\Omega_Z^i]_{t-h/2}}{[1 - h^2\{\sigma_Y\sigma_Z\Omega_X^i{}^2 + \sigma_X\sigma_Z\Omega_Y^i{}^2 + \sigma_X\sigma_Y\Omega_Z^i{}^2\} - 2h^3\sigma_X\sigma_Y\sigma_Z\Omega_X^i\Omega_Y^i\Omega_Z^i]_{t+h/2}}. \quad (27)$$

Therefore, unless  $J_X = J_Y = J_Z$ , the single discrete step within our algorithm is not volume conserving, i.e.,  $\mathcal{J}_{\Omega_i}(t) = 1 + \mathcal{O}(h^3)$ . However, since principal angular velocities are Gaussian distributed in equilibrium with  $\langle \Omega_X^i \Omega_Y^i \Omega_Z^i \rangle = \langle \Omega_X^i \rangle \langle \Omega_Y^i \rangle \langle \Omega_Z^i \rangle = 0$ , the overall Jacobian  $\mathcal{J}_{\mathcal{N}} = \prod_n^{\mathcal{N}} \mathcal{J}_{\Omega_i}(t + nh)$  will fluctuate around unity. Moreover, the probability of deviations of  $\mathcal{J}_{\mathcal{N}}$  from unity on some value  $u$  will decrease rapidly (as  $1/\exp(\sim u/h^3)$ ) with increasing  $u$  and will not depend on the total time step  $\mathcal{N}$  performed. In other words, such deviations are not accumulated during the integration.

From the afore said, it becomes clear that to reduce the fluctuations of  $\mathcal{J}_{\Omega_i}(t)$  to zero, it is necessary to take into account the contributions  $(J_\beta - J_\gamma)\Omega_\beta^i \Omega_\gamma^i \equiv [\mathbf{W}(\Omega_i)\mathbf{J}\Omega_i]_\alpha$  of free-motion torques into the angular-velocity dynamics more precisely (here  $\mathbf{J}$  denotes the diagonal matrix of principal moments of inertia). To do this, let us write the solutions  $\Omega_i(t + \frac{h}{2})$  to Eq. (6) in the following formal form  $\hat{\mathcal{S}}(h)\Omega_i(t - \frac{h}{2})$ , where  $\hat{\mathcal{S}}(h)$  is a velocity-displacement operator. It is obvious by construction that  $\lim_{s \rightarrow \infty} [\hat{\mathcal{S}}(h/s)]^s = e^{Lh}$ , where  $L = \mathbf{J}^{-1}[\mathbf{K}_i + \mathbf{W}(\Omega_i)\mathbf{J}\Omega_i]\partial/\partial\Omega_i$  is a part of the Liouville operator of the system, so that  $d\Omega_i/dt = L\Omega_i$ . Of course, the evolution operator  $e^{Lh}$  does not lead, in general, to exact solutions, since the torque caused by potential forces is assumed to be constant,  $\mathbf{K}_i \equiv \mathbf{K}_i(t)$ , over the time interval  $[t - \frac{h}{2}, t + \frac{h}{2}]$ . Thus like  $\hat{\mathcal{S}}(h)$ , the propagator  $e^{Lh}$  generates new angular velocities with the same  $\mathcal{O}(h^3)$  order local errors. However, the operator  $L$  allows to be decomposed into a sum  $L_1 + L_2$ , and then the (Trotter) formula  $e^{Lh} = e^{L_2 \frac{h}{2}} e^{L_1 h} e^{L_2 \frac{h}{2}} + \mathcal{O}(h^3)$  can be used to approximate the full propagator. Although different decompositions are possible, it is essential for our purposes, to decompose  $L$  in such a way to solve the problem analytically.

The last requirement leads to the following decomposition

$$L_1 = \mathbf{J}^{-1}\mathbf{K}_i \frac{\partial}{\partial\Omega_i}, \quad L_2 = \mathbf{J}^{-1}\mathbf{W}(\Omega_i)\mathbf{J}\Omega_i \frac{\partial}{\partial\Omega_i}. \quad (28)$$

Then  $e^{L_1 h}\Omega_i = \Omega_i + h\mathbf{J}^{-1}\mathbf{K}_i$ , whereas the propagator  $e^{L_2 h/2}$  corresponds to a free rotational dynamics. As is well known, Euler equations (4) are integrated analytically in this case. Let  $\frac{1}{2}\sum_\alpha^{X,Y,Z} J_\alpha \Omega_\alpha^2 = \mathcal{H}$  and  $\frac{1}{2}\sum_\alpha^{X,Y,Z} J_\alpha^2 \Omega_\alpha^2 = \mathcal{M}^2$  be the kinetic energy and square angular momenta of a body, associated with angular velocity  $\Omega$ ,  $j_\alpha = \frac{1}{2}(-\sigma_\beta \sigma_\gamma)^{-1/2}$ ,  $\varepsilon = [(J_Z - J_Y)(\mathcal{M}^2 - 2\mathcal{H}J_X)/J_X J_Y J_Z]^{1/2}$  and  $\kappa = [(J_Y - J_X)(2\mathcal{H}J_Z - \mathcal{M}^2)/((J_Z - J_Y)(\mathcal{M}^2 - 2\mathcal{H}J_X))]^{1/2}$ . Then, the result for transformed angular velocities  $\Omega' = e^{L_2 h/2}\Omega$  can be presented in the form [47]:



$$\begin{aligned}
\Omega'_X &= \kappa j_X \varepsilon \operatorname{cn}(\varepsilon \frac{h}{2} + v), \\
\Omega'_Y &= \operatorname{sign}(\Omega_Z) \kappa j_Y \varepsilon \operatorname{sn}(\varepsilon \frac{h}{2} + v), \\
\Omega'_Z &= \operatorname{sign}(\Omega_Z) j_Z \varepsilon \operatorname{dn}(\varepsilon \frac{h}{2} + v),
\end{aligned} \tag{29}$$

where  $\operatorname{sign}(x)$  denotes sign of  $x$ ,  $\operatorname{dn}(x) = [1 - \kappa^2 \sin^2(\operatorname{am}(x))]^{1/2}$ ,  $\operatorname{sn}(x) = \sin(\operatorname{am}(x))$  and  $\operatorname{cn}(x) = \cos(\operatorname{am}(x))$  are Jacobian elliptic functions [48], so that  $\Xi(\operatorname{am}(x), \kappa) = \int_0^{\operatorname{am}(x)} d\psi / [1 - \kappa^2 \sin^2 \psi]^{1/2} = x$  with  $\Xi$  being a Legendre elliptic integral of the first kind (the program code for these functions can be found in [49]). The constant  $v$  is determined from the initial boundary condition  $\lim_{h \rightarrow 0} \boldsymbol{\Omega}' = \boldsymbol{\Omega}$ , which leads to  $v = \bar{v} \operatorname{sign}(\Omega_Y \Omega_Z \operatorname{sn}(\bar{v}))$ , where  $\bar{v} = \Xi(\arccos(\Omega_X / (j_X \kappa \varepsilon)), \kappa)$ . Note that analytical solutions (29) are applicable when  $\mathcal{M}^2 \geq 2\mathcal{H}J_Y$ . Otherwise, the indexes  $X$  and  $Z$  should be replaced between themselves in Eq. (29) and in expressions for  $\varepsilon$ ,  $\kappa$  and  $v$ .

It can be checked directly that the Jacobian of transformation  $\boldsymbol{\Omega}' = e^{L_2 h/2} \boldsymbol{\Omega}$  is equal to unity. This valid also for the operator  $e^{L_1 h}$ , because a simple shift does not change the volume. Therefore, if the angular velocities are integrated, instead of (6), as

$$\boldsymbol{\Omega}_i(t + \frac{h}{2}) = e^{L_2 \frac{h}{2}} e^{L_1 h} e^{L_2 \frac{h}{2}} \boldsymbol{\Omega}_i(t - \frac{h}{2}), \tag{30}$$

our algorithm will be symplectic in rigorous meaning.

## F. Integration in specific cases

Although the algorithm described can be applied to arbitrary rigid polyatomics, some simplifications are possible using special properties of the molecule. The simplest case is molecules with a spherical distribution of mass, when  $J_X = J_Y = J_Z \equiv J$ . Then, no free-motion torques appear, and it is more convenient to work within the body-vector representation and to rewrite equations (1) and (4) in terms of angular velocities  $\boldsymbol{\omega}_i = \mathbf{A}_i^+ \boldsymbol{\Omega}_i$  in the laboratory frame, i.e.,  $d\mathbf{A}_i/dt = \mathbf{A}_i \mathbf{W}(\boldsymbol{\omega}_i)$  and  $J d\boldsymbol{\omega}_i/dt = \mathbf{k}_i - \lambda J \boldsymbol{\omega}_i$ . The leapfrog trajectories for these equations are obvious:  $\boldsymbol{\omega}_i(t + \frac{h}{2}) = [\nu_-(t) \boldsymbol{\omega}_i(t - \frac{h}{2}) + \frac{h}{J} \mathbf{k}_i(t)] / \nu_+(t)$  and  $\mathbf{A}_i(t + h) = \mathbf{A}_i(t) \exp[\varphi_i \mathbf{W}(\boldsymbol{\omega}_i) / \omega_i]_{t+\frac{h}{2}}$ , where  $\varphi_i = \arcsin[h\omega_i / (1 + \frac{h^2}{4}\omega_i^2)]_{t+\frac{h}{2}}$ .

For some particular models, the orientational part of intermolecular potentials can be expressed using only unit vectors  $\boldsymbol{\rho}_i$  passing through the centers of mass of

molecules. The examples are point dipole interactions, when  $\boldsymbol{\rho}_i \equiv \boldsymbol{\nu}_i/\nu_i$  with  $\boldsymbol{\nu}_i$  being the dipole moment, or when all force sites of the molecule are aligned along  $\boldsymbol{\rho}_i$ . If then additionally the condition  $J_{X,Y,Z} = J$  is satisfied (for the last example this can be possible when forceless mass sites are placed in such a way to ensure this condition), it is no longer necessary to deal with orientational matrices or quaternions. In this case the equation for  $\boldsymbol{\rho}_i$  looks as  $d\boldsymbol{\rho}_i/dt = \mathbf{W}^+(\boldsymbol{\omega}_i)\boldsymbol{\rho}_i$  with the solution  $\boldsymbol{\rho}_i(t+h) = \exp[-\varphi_i \mathbf{W}(\boldsymbol{\omega}_i)/\omega_i]_{t+\frac{h}{2}} \boldsymbol{\rho}_i(t)$ .

For molecules with the cylindric symmetry of mass distribution, the numerical trajectory can also be determined in a simpler manner. Let us assume for definiteness that  $J_X = J_Y \neq J_Z \neq 0$ . Then arbitrary two perpendicular between themselves axes, lying in the plane perpendicular to  $Z$ -th principal axis, can be chosen initially as  $X$ - and  $Y$ -th principal orths. The corresponding solution to Eq. (17) at  $\alpha = Z$  is found now exactly, namely,  $\Omega_Z^i(t + \frac{h}{2}) = [\nu_-(t)\Omega_Z^i(t - \frac{h}{2}) + \frac{h}{J_Z}K_Z^i(t)]/\nu_+(t)$  (the  $X$ - and  $Y$ -th components are obtained automatically in view of Eq. (20)), whereas the orientational matrices or quaternions are computed via Eq. (11).

A special attention should be paid on linear molecules when  $J_X = J_Y = J \neq J_Z = 0$ . Each such molecule has two orientational degrees of freedom and to reproduce a correct dynamics by Euler equations it is necessary to putt formally  $\Omega_Z^i \equiv 0$  to exclude nonexisting torques caused by irrelevant rotations of the molecule around  $Z$ -axis. Then, it follows from Eq. (20) that  $\Omega_{X,Y}^i(t + \frac{h}{2}) = [\nu_-(t)\Omega_{X,Y}^i(t - \frac{h}{2}) + \frac{h}{J}K_{X,Y}^i(t)]/\nu_+(t)$ . Planar molecules do not present a specific case within our approach and they are handled as tree-dimensional bodies.

### III. MD TESTS. COMPARISON WITH PREVIOUS METHODS

The system chosen was the TIP4P model of water [50] at a density of  $mN/V = 1$  g/cm<sup>3</sup> and temperature of  $T = 298$  K. Such a system should provide a very severe test for rotational algorithms because of the low moments of inertia of the molecule and the large torques due to the site-site interactions. To reduce cut-off effects we used a cubic sample of  $N = 256$  molecules and the reaction field geometry [51]. Our MD programs were implemented using Fortran language and double precision throughout. They were executed on a Pentium-S 120 MHz personal computer at around 0.8 s per

time step. All runs were started from an identical well equilibrated configuration.

We have made comparative tests on the basis of our advanced leapfrog algorithm, the implicit leapfrog algorithm of Fincham [26], pseudo-site formalism [23], angular-velocity Verlet method within matrix- and quaternion-constraint schemes [27, 28], and the atomic-constraint technique [17, 18]. The results obtained for the total energy fluctuations  $\mathcal{E} = [(\langle E - \langle E \rangle)^2]^{1/2}/|\langle E \rangle|$  as functions of the length ( $\mathcal{N} = t/h$ ) of the microcanonical (NVE) simulations are shown in Fig. 1 at four fixed step sizes,  $h = 1, 2, 3$  and 4 fs (a step size of 2 fs is normally used [52, 53] to simulate water within the atomic-constraint approach). As can be seen, the Fincham’s leapfrog (marked simply as ”leapfrog“ in Fig. 1) and pseudo-site schemes appear to be unstable already for the least time step considered and they lead to the worst energy conservation. Much more stable trajectories are produced by the velocity-Verlet integrator within quaternion- and matrix-constraint schemes which exhibit similar equivalence in the energy conservation. But the results are rather poor at moderate and great time steps ( $h \geq 3$  fs). Only the atomic-constraint and our advanced leapfrog algorithms can be related to long-term stable schemes.

We mention that the computation of total energy  $E = T + U$  (consisting of kinetic  $T$  and potential  $U$  parts) at time  $t$  within the leapfrog framework requires the knowledge of on-step velocities. These velocities can be calculated using usual estimators (14) and (16). The corresponding curves of dependencies  $\mathcal{E}(\mathcal{N})$  are labeled by ”1“ in Fig. 1. They are almost identical to those obtained within the atomic-constraint technique. Note that  $\mathcal{O}(h^2)$  uncertainties, arising in evaluations (14) and (16), are in the self-consistency with second-order global errors appearing during the leapfrog integration. Despite this, an additional portion is involved into the main  $\mathcal{O}(h^2)$  term of accumulated errors for  $\mathcal{E}$ , increasing the total energy fluctuations with no relation to the real accuracy of the computed trajectory [54]. Although various more accurate estimators are available [55], we have established that the following four-point symmetric scheme

$$\mathbf{V}(t) = \frac{1}{16} \left[ -\mathbf{V}(t - \frac{3h}{2}) + 9\mathbf{V}(t - \frac{h}{2}) + 9\mathbf{V}(t + \frac{h}{2}) - \mathbf{V}(t + \frac{3h}{2}) \right] + \mathcal{O}(h^4), \quad (31)$$

where  $\mathbf{V} \equiv \{\mathbf{v}_i, \boldsymbol{\Omega}_i\}$ , leads to the best energy conservation within our leapfrog algorithm. It is understood, of course, that mid-step velocities entering into the right-hand site of Eq. (31) are already defined quantities. Thus, the computation of the total

energy  $E$  at time  $t$  becomes possible, when the velocity step  $t + \frac{3h}{2}$  has been passed and the potential energy  $U(t)$  (known at this stage already at  $t + h$ ) has been taken from memory. The corresponding dependencies of  $\mathcal{E}$  on  $\mathcal{N}$  are plotted in Fig. 1 by the boldest (lowest lying) curves marked as "2". In this case, the total-energy fluctuations decrease about in 1.5 times with respect to the usual two-point scheme.

The quaternion and principal-axis representations of the advanced leapfrog algorithm conserved the energy approximately with the same accuracy. For this reason, the result concerning principal-axis variables is not plotted in Fig. 1 to simplify the graph. The leapfrog trajectories were generated applying quasianalytical solutions (Eqs. (20) and (26)) for angular velocities. The solutions obtained by means of iterations of Eq. (6) were calculated also for comparison. No deviations between the both results have been identified up to  $h = 6$  fs. They differed on each step by uncertainties of order round-off errors only, so that the free-of-iteration scheme appears to be in an excellent accord. No shift of the total energy and temperature was observed during the advanced leapfrog trajectories at  $h \leq 5$  fs over a length of 10 000 time steps. The deviations from unity of the overall Jacobian  $\mathcal{J}_{\mathcal{N}}$  (see Eq. (27)) never exceed about 5% (at  $h \leq 4$  fs).

Finally, the rigorously symplectic version (30) has also been examined (the longest-dashed curves in Fig. 1) within the four-point scheme (31). As we can see, this version does not lead to improvements in energy conservation, despite the fact that the free-motion propagator  $e^{L_2h/2}$  is evaluated exactly. This is so because for water at the given thermodynamic point, the free-motion torques are much smaller in amplitude with respect to the torques caused by interactions. An increased conservation of energy can be expected for systems at high temperatures, where the free-motion contributions into the torques become dominate. Otherwise, the analytical version (29) is not generally recommended because it requires the calculation of somewhat time-consuming elliptic functions (although we did not observe any considerable decreasing time efficient, given that near 95% of the total computer time were spent to evaluate pair interactions). In the limiting case when the potential-force torques are absent at all, symplectic solutions (29) will lead to exact results with automatic preservation of energy and angular momenta. The symplectic version should also be used in situations where a precise conservation of the volume in phase space at each time step is very important.

It is worth remarking that the variant  $L_1 \leftrightarrow L_2$  of decomposition (28) in transformation (30) is also acceptable in view of the symplecticity. We have established, however, that such a decomposition leads to worse energy conservation in our simulations (probably because of  $\langle \mathbf{K}_i^2 \rangle \gg \langle [\mathbf{W}(\boldsymbol{\Omega}_i)\mathbf{J}\boldsymbol{\Omega}_i]^2 \rangle$ ).

To properly reproduce features of NVE ensembles, it is necessary for the ratio  $\Upsilon$  of  $\mathcal{E}$  to the fluctuations  $\mathcal{U}$  of potential energy to be no more than a few per cent. We have obtained the following levels of  $\mathcal{E}$  (within the two-point scheme) at the end of these trajectories: 0.0016, 0.0065, 0.015, 0.029, 0.049 and 0.10 %, corresponding to  $\Upsilon \approx 0.29, 1.2, 2.7, 5.2, 8.7$  and 18 % at  $h = 1, 2, 3, 4, 5$  and 6 fs, respectively ( $\mathcal{U} \approx 0.56\%$  for the system under consideration). Therefore, a step size of 4 fs is still suitable for precise calculations. The greatest time steps 5 fs and 6 fs can sometimes be acceptable when the precision is not so important, for example, for the equilibration of configurations. The ratio  $\Upsilon$  in the interval  $h \leq 5$  fs can be fitted with a great accuracy to the function  $Ch^2$  with the coefficient  $C \approx 0.29 \text{ \% fs}^{-2}$ . This is completely in line with the square growth of global errors appearing during the integration by Verlet-type integrators [54].

To verify the angular-velocity approach in more detail, in our NVE and canonical (NVT) ensemble simulations we measured besides the total energy and temperature some other relevant functions of the system, namely, specific heat at constant volume, mean-square forces and torques, oxygen-oxygen and hydrogen-hydrogen radial distribution functions (RDFs). Center-of-mass (CM) and angular-velocity (AV) time autocorrelation functions (TAFs) were also found. Orientational relaxation was studied by evaluating the molecular dipole-axis (DA) autocorrelations. The NVE simulations, performed within the atomic-constraint technique at  $h = 2$  fs, was considered as a benchmark against which other algorithms and step sizes are to be compared. First of all, to finish the discussion with the NVE integrators, we report that deviations in all the measured functions with respect to their benchmark values were in a complete agreement with the corresponding relative fluctuations  $\Upsilon$ . For example, the results obtained with the help of the advanced leapfrog algorithm at  $h = 2$  fs were indistinguishable from the benchmark ones. At the same time, they differed as large as around 5%, 10% or even 20% with increasing the time step to 4 fs, 5 fs or 6 fs, respectively, however, these differences were smaller than for other integrators. Therefore, there is a little point in pursuing the energy-conserving algorithms to time steps larger than 4

fs because the deviations become evident.

In the case of NVT simulations, the investigated quantities were less sensitive to the step size increasing. These simulations have been performed using the Fincham implicit algorithm [26] (within the Brown and Clarke thermobath [37]) as well as the advanced leapfrog integrator within the N ose-Hoover thermostat (Sec. II C) applying the free-of-iteration scheme (Eqs. (20) and (26)). The thermostat relaxation time  $\tau$  was chosen to be 1 ps, (i.e.,  $h \ll \tau \ll \mathcal{N}h$ ) and the friction coefficient  $\lambda(t)$  was putted to be zero at the very beginning ( $t = 0$ ) of the simulations. The RDFs and CM, AV and DA TAFs calculated during the NVT integrations at different step sizes ( $h = 2\text{--}10$  fs) are shown in Fig. 2 in comparison with the benchmark results. These functions at  $h = 4$  and 6 fs coincided completely with those corresponding to  $h = 2$  fs and they are not shown in subsets (a)–(b) to simplify the presentation. As can be seen from Fig. 2, the RDFs remain practically the same at  $h \leq 8$  fs in the case of the advanced integrator. The deviations of all the correlation functions from the benchmark within the usual implicit algorithm are clearly larger. The orientational correlation function (see subset (d)) is to show a systematic discrepancy in this case. For instance, these deviations at  $h = 4$  fs are as big as those obtained during the advanced leapfrog integration at  $h = 8$  fs. Therefore, the last approach allows a step size approximately twice larger than the usual implicit integrator. We conclude, therefore, that the thermostatted advanced leapfrog integrator allows to be used up to a time step of 6 fs, given that then there is no difference in RDFs, while CM, AV and DA TAFs are also close.

#### IV. CONCLUDING REMARKS

We have formulated a new approach for numerical integration of the equations of motion for systems with interacting rigid bodies. Unlike other standard methods, the principal angular velocities are involved directly into the integration within this approach. The algorithm derived is categorized as a rotational leapfrog, since the variables saved are mid-step angular velocities and on-step orientational positions. The orientations can be expressed in terms of either quaternions or entire rotational matrices. The interpolation of velocity- and orientation-dependent quantities to the corresponding middle time points was carried out using a simple averaging over the

two nearest neighboring values that is in the spirit of the leapfrog idea as well. As a result, the following significant benefits have been achieved: (i) the exact conservation of rigid structures appears to be an intrinsic feature of the algorithm, and (ii) all the evaluations are performed analytically in both NVE and NVT ensembles without involving any iterative procedures.

It has been shown on the basis of an actual computer experiment on water that the algorithm presented exhibits better energy conserving properties than those observed in all other rigid-motion integrators known. The algorithm can easily be implemented for arbitrary rigid bodies and substituted into existing program codes. It seems to be a good alternative to the atomic-constraint method in the case of long term MD simulations of systems with rigid polyatomic molecules.

The approach introduced can be developed to perform a MTS integration within the RESP technique. This question will be considered in our further studying. Some ideas of the MTS integration have already be used in this paper to derive symplectic versions of the advanced leapfrog algorithm. The reformulation of the RESP approach in generalized coordinates containing translational and orientational variables explicitly may lead to significant simplifications when selecting efficient reference system propagators. For example, translational motions (which are much slower than rotational ones for the most of liquids) can be decomposed directly within such coordinates. The most notorious demonstration is very fast rotations of rigid bodies in the inertial-motion regime. Then for molecules with a spherically symmetric distribution of mass we merely obtain  $\mathbf{v}_i = \text{const}$  and  $\mathbf{\Omega}_i = \text{const}$  within the molecular approach. To reproduce such a behavior within the atomic technique, it is necessary to integrate (with a very small step size) the equations of motion in the presence of rapidly varying strong constraint forces. The decomposition of rotational propagators containing interactions into slow and fast parts can also be done easily splitting in an appropriate way the free-motion and potential-force torques.

**Acknowledgements.** This work was financially supported in part by a grant of the President of Ukraine. I wish to thank Dr. A. Duviryak for helpful discussions. I would like also to thank Professor B.J. Berne and Professor G.J. Martyna for sending me reprints of some articles.

## REFERENCES

- [1] H. Goldstein, *Classical Mechanics*, (Addison-Wesley, Reading, Massachusetts, 1980).
- [2] J. Barojas, D. Levesque, and B. Quentrec, Simulation of diatomic homonuclear liquids, *Phys. Rev. A* **7**, 1092 (1973).
- [3] D. Levesque, J.J. Weis, and G.N. Patey, Fluids of Lennard-Jones spheres with dipoles and tetrahedral quadrupoles. A comparison between computer simulation and theoretical results, *Mol. Phys.* **51**, 333 (1984).
- [4] D.J. Evans, On the representation of orientation space, *Mol. Phys.* **34**, 317 (1977).
- [5] M.P. Allen and D.J. Tildesley, *Computer Simulation of Liquids* (Oxford Science Press, Oxford, 1987).
- [6] D.C. Rapaport, *The Art of Molecular Dynamics Simulation* (Cambridge University Press, Cambridge, 1995).
- [7] C.W. Gear, *Numerical Initial Value Problems in Ordinary Differential Equations* (Prentice-Hall, Engelwood Cliffs, NJ, 1971).
- [8] A. Rahman and F.H. Stillinger, Molecular dynamics study of liquid water, *J. Chem. Phys.* **55**, 3336 (1971).
- [9] D.J. Evans and S. Murad, Singularity free algorithm for molecular dynamics simulation of rigid polyatomics, *Mol. Phys.* **34**, 327 (1977).
- [10] J.P. Ryckaert and A. Bellemans, Molecular dynamics of liquid *n*-butane near its boiling point, *Chem. Phys. Lett.* **30**, 123 (1975).
- [11] G. Ciccotti and J.P. Ryckaert, Molecular dynamics simulation of rigid molecules, *Comput. Phys. Rep.* **4**, 345 (1986).
- [12] L. Verlet, Computer experiments on classical fluids. I. Thermodynamic properties of Lennard-Jones molecules, *Phys. Rev.* **159**, 98 (1967).
- [13] W.C. Swope, H.C. Andersen, P.H. Berens, and K.R. Wilson, A computer simulation method for the calculation of equilibrium constants for the formation of physical clusters of molecules: Application to small water clusters, *J. Chem. Phys.* **76**, 637 (1982).
- [14] R.W. Hockney and J.W. Eastwood, *Computer Simulation Using Particles* (McGraw-Hill, New York, 1981).
- [15] D. Beeman, Some multistep methods for use in molecular dynamics calculations, *J. Comput. Phys.* **20**, 130 (1976).
- [16] G.D. Venneri and W.G. Hoover, Simple exact test for well-known molecular dynamics algorithms, *J. Comput. Phys.* **73**, 486 (1987).
- [17] J.P. Ryckaert, G. Ciccotti, and H.J.C. Berendsen, Numerical integration of the Cartesian equations of motion of a system with constraints: Molecular dynamics of *n*-alkanes, *J. Comput. Phys.* **23**, 327 (1977).
- [18] G. Ciccotti, M. Ferrario, and J.P. Ryckaert, Molecular dynamics of rigid systems in cartesian coordinates. A general formulation, *Mol. Phys.* **47**, 1253 (1982).



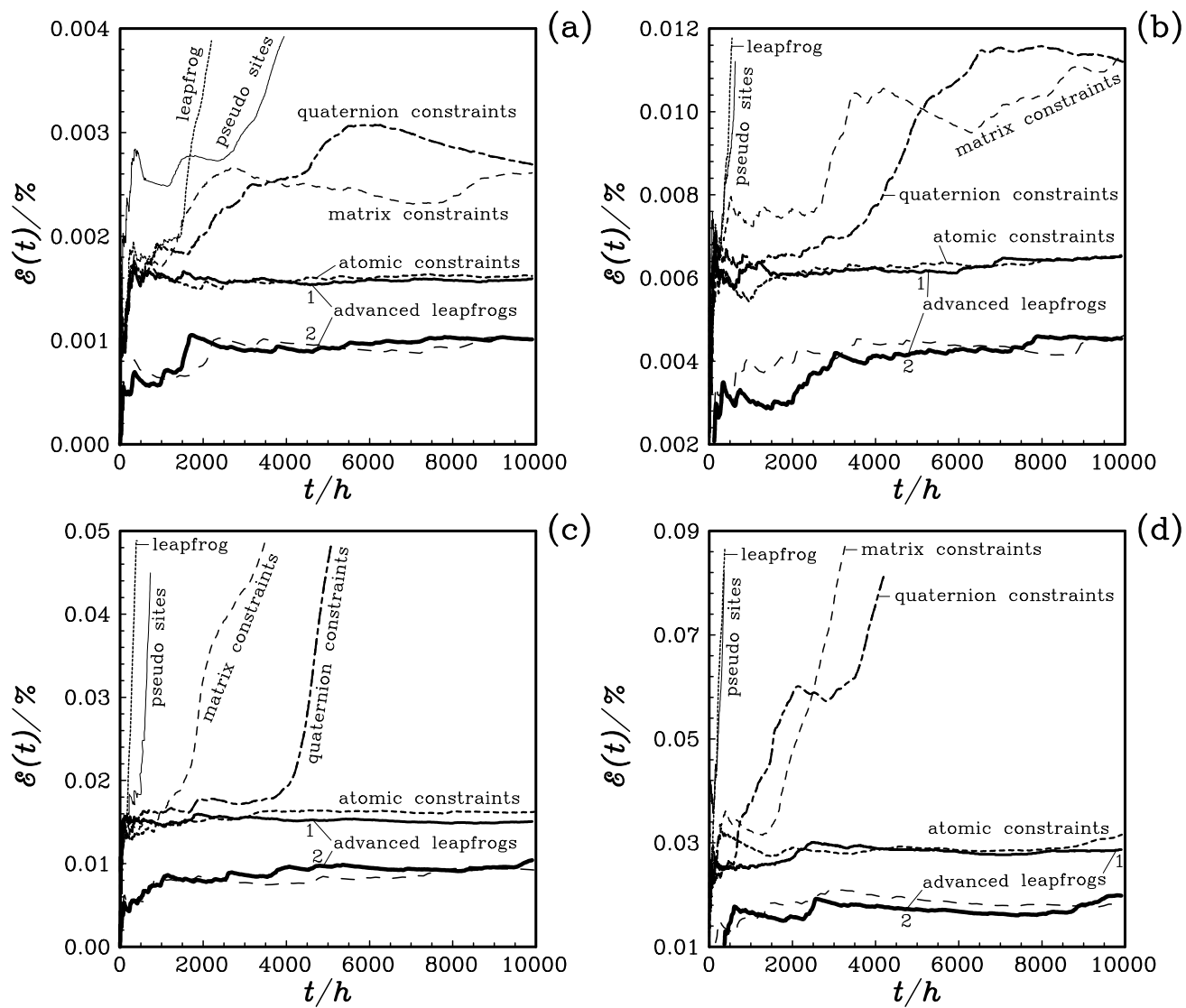
- [19] H.C. Andersen, Rattle: a ‘velocity’ version of the shake algorithm for molecular dynamics calculations, *J. Comput. Phys.* **52**, 24 (1983).
- [20] M. Ferrario and J.P. Ryckaert, Constant pressure-constant temperature molecular dynamics for rigid and partially rigid molecular systems, *Mol. Phys.* **54**, 587 (1985).
- [21] B.J. Leimkuhler and R.D. Skeel, Symplectic numerical integrators in constrained Hamiltonian systems, *J. Comput. Phys.* **112**, 117 (1994).
- [22] E. Barth, K. Kuczera, B. Leimkuhler, and R. D. Skeel, Algorithms for constrained molecular dynamics, *J. Comput. Chem.* **16**, 1192 (1995).
- [23] R. Ahlrichs, and S. Brode, A new rigid motion algorithm for MD simulations, *Comput. Phys. Commun.* **42**, 59 (1986).
- [24] A. Kol, B. Laird, and B. Leimkuhler, A symplectic method for rigid-body molecular simulation, in Numerical Analysis Reports (University of Cambridge, DAMTP 1997/NA5).
- [25] D. Fincham, An algorithm for the rotational motion of rigid molecules, *CCP5 Information Quarterly* **2**, 6 (1981).
- [26] D. Fincham, Leapfrog rotational algorithms, *Mol. Simul.* **8**, 165 (1992).
- [27] I.P. Omelyan, Numerical integration of the equations of motion for rigid polyatomics: The matrix method, *Comput. Phys. Commun.* **109**, 171 (1998).
- [28] I.P. Omelyan, On the numerical integration of motion for rigid polyatomics: The modified quaternion approach, *Computers in Physics* **12**, 97 (1998).
- [29] M.E. Tuckerman, G.J. Martyna, and B.J. Berne, Molecular dynamics algorithm for condensed systems with multiple time scales, *J. Chem. Phys.* **93**, 1287 (1990).
- [30] M. Tuckerman, B.J. Berne, and A. Rossi, Molecular dynamics for multiple time scales: Systems with disparate masses, *J. Chem. Phys.* **94**, 1465 (1991).
- [31] M. Tuckerman, G.J. Martyna, and B.J. Berne, Molecular dynamics algorithms for multiple time scales: Systems with long range forces, *J. Chem. Phys.* **94**, 6811 (1991).
- [32] M. Tuckerman, B.J. Berne, and G.J. Martyna, Reversible multiple time scale molecular dynamics, *J. Chem. Phys.* **97**, 1990 (1992).
- [33] S.J. Stuart, R. Zhou, and B.J. Berne, Molecular dynamics with multiple time scales: The selection of efficient reference system propagators, *J. Chem. Phys.* **105**, 1426 (1996).
- [34] G.J. Martyna, M. Tuckerman, D.J. Tobias, and M.L. Klein, Explicit reversible integrators for extended systems dynamics, *Mol. Phys.* **87**, 1117 (1996).
- [35] I.P. Omelyan, Multiple time scale molecular dynamics in orientational space, (unpublished).
- [36] I.P. Omelyan, Algorithm for numerical integration of the rigid-body equations of motion, *Phys. Rev. E* **58**, 1169 (1998).
- [37] D. Brown and J.H.R. Clarke, A comparison of constant energy, constant temperature and constant pressure ensembles in molecular dynamics simulations of atomic liquids, *Mol. Phys.* **51**, 1243 (1984).

- [38] H.J.C. Berendsen, J.P.M. Postma, W.F. van Gunsteren, A. di Nicola, and J.R. Haak, Molecular dynamics with coupling to an external bath, *J. Chem. Phys.* **81**, 3684 (1984).
- [39] S. N ose, A molecular dynamics method for simulation in the canonical ensemble, *Mol. Phys.* **52**, 255 (1984).
- [40] W.G. Hoover, Canonical dynamics: Equilibrium phase-space distributions, *Phys. Rev. A* **31**, 1695 (1985).
- [41] S. N ose, Constant temperature molecular dynamics methods, *Progs. Theor. Phys. Supp.* **103**, 1 (1991).
- [42] S. Melchionna, G. Ciccotti and B.L. Holian, Hoover’s style Molecular Dynamics for systems varying in shape and size, *Mol. Phys.* **78**, 533 (1993).
- [43] G.J. Martyna, M.L. Klein, M. Tuckerman, Nose-Hoover chains: The canonical ensemble via continuous dynamics, *J. Chem. Phys.* **97**, 2635 (1992).
- [44] D. Fincham, Choice of time step in molecular dynamics simulations, *Comput. Phys. Commun.* **40**, 263 (1986).
- [45] S. Toxvaerd, Molecular dynamics at constant temperature and pressure, *Phys. Rev. E* **47**, 343 (1993).
- [46] D. Frenkel and B. Smit, Understanding Molecular Simulation: from Algorithms to Applications (Academic Press, New York, 1996).
- [47] A.M. Lyapunov, Lectures in Theoretical Mechanics (Naukova Dumka, Kiev, 1982) [in Russian]; see also L. D. Landau and E. M. Lifshitz, Mechanics, 3rd edn (Pergamon Press, New York, 1978).
- [48] M. Abramowitz and I.A. Stegun (Eds.), Handbook of Mathematical Functions, Applied Mathematics Series, Vol. 55 (National Bureau of Standards, Washington, 1964).
- [49] W.H. Press, S.A. Teukolsky, W.T. Vetterling, and B.P. Flannery, Numerical Recipes in Fortran 77. The Art of Scientific Computing, 2nd edn, Vol. 1 (Cambridge University Press, Cambridge, 1992).
- [50] W.L. Jorgensen, J. Chandrasekhar, J.D. Madura, R.W. Impey, and M.L. Klein, Comparison of simple potential functions for simulating liquid water, *J. Chem. Phys.* **79**, 926 (1983).
- [51] I.P. Omelyan, On the reaction field for interaction site models of polar systems, *Phys. Lett. A* **223**, 295 (1996).
- [52] D. Bertolini and A. Tani, Generalized hydrodynamics and the acoustic modes of water: Theory and simulation results, *Phys. Rev. E* **51**, 1091 (1995).
- [53] A. K. Mazur, Hierarchy of fast motions in protein dynamics, *J. Phys. Chem. B* **102**, 473 (1998).
- [54] A.K. Mazur, Common molecular dynamics algorithms revisited: Accuracy and optimal time steps of St ormer-leapfrog integrators, *J. Comput. Phys.* **136**, 354 (1997).
- [55] M. Amini and D. Fincham, Evaluation of temperature in molecular dynamics simulation, *Comput. Phys. Commun.* **56**, 313 (1990).

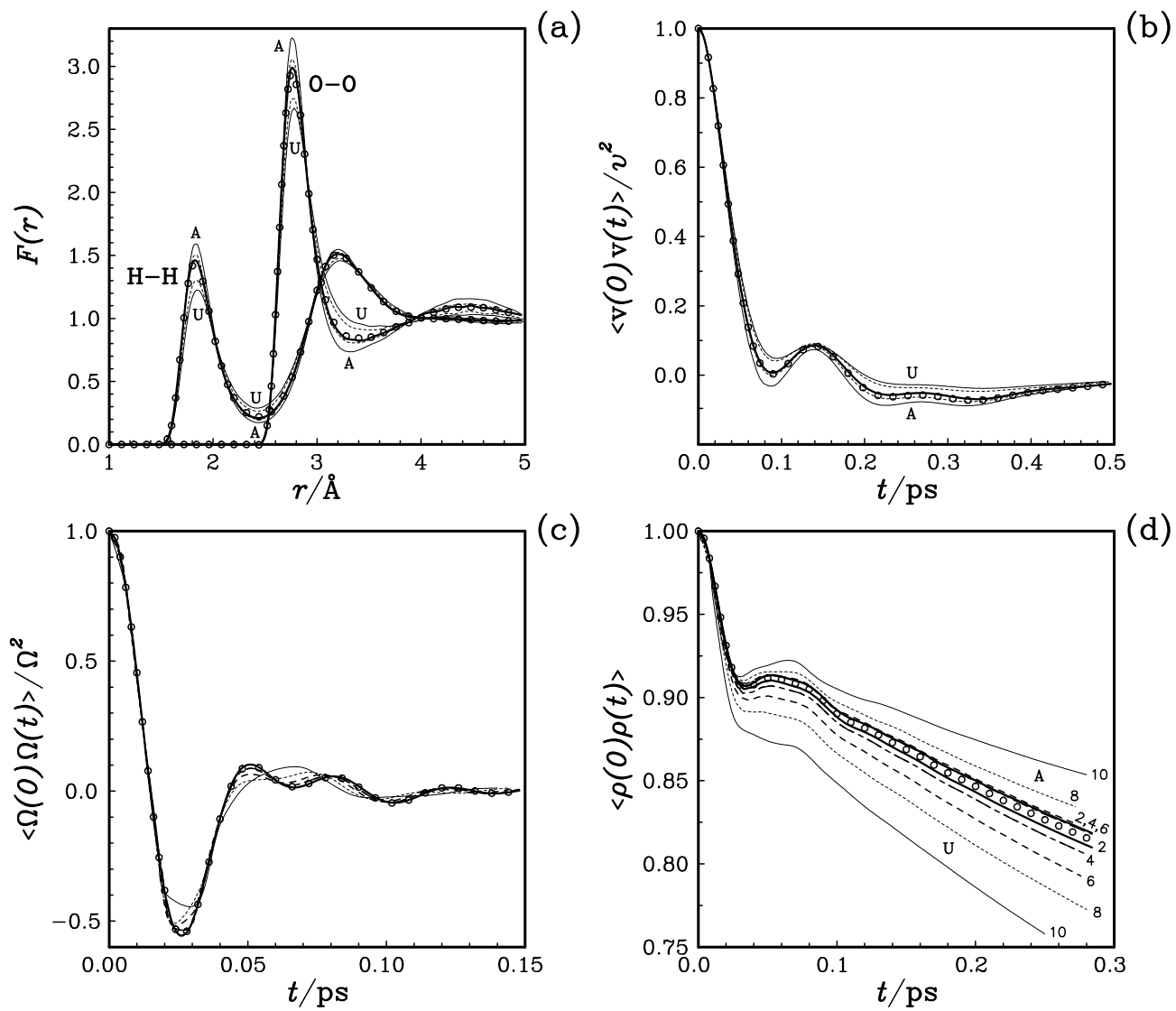
## Figure captions

Fig. 1. The total energy fluctuations as functions of the length of the NVE simulations on the TIP4P water, performed in various techniques at four fixed time steps: **(a)** 1 fs, **(b)** 2 fs, **(c)** 3 fs and **(d)** 4 fs.

Fig. 2. Oxygen-oxygen (O-O) and hydrogen-hydrogen (H-H) radial distribution functions **(a)**, center-of-mass **(b)** and angular-velocity **(c)** time autocorrelation functions, and orientational relaxation **(d)**, obtained in the NVT simulations of the TIP4P water. The results corresponding to the step sizes  $h = 2, 8$  and  $10$  fs are plotted by bold solid, short-dashed and thin solid curves, respectively. Additional long-short dashed and dashed curves in **(c)**–**(d)** correspond to the cases of  $h = 4$  and  $6$  fs. The sets of curves related to the usual implicit and advanced leapfrog algorithms are labeled by "U" and "A", respectively (the result of the usual implicit algorithm is not included in **(c)** to simplify the graph). The benchmark data are shown as open circles. Note that the advanced-algorithm curves are indistinguishable in **(d)** at  $h = 2, 4$  and  $6$  fs.



*Fig. 1. I.P.Omelyan*  
*Journal of Computational Physics*



*Fig. 2. I.P.Omelyan*  
*Journal of Computational Physics*